2 Measuring the universe

We have seen so far that the cosmological model is expressed is highly geometric terms, i.e. a homogeneous and isotropic line element defined by a time varying scale factor and a spatial curvature term. Correspondingly, tests of the cosmological model are highly geometric in nature. The basic aim of many of these tests is to relate quantities based upon the metric (e.g. distance and volume) to the **sole cosmological observable – redshift**. Note that in the previous lecture we discussed very broad tests/observations of cosmological model, i.e. total mass density and age. In contrast to this, the tests we will discuss today all aim to constrain the cosmological model via the behaviour of the metric. Two concepts will dominate the discussion;

1. Using the RW metric to determine distance, time and volume as a function of redshift in the universe.

2. Isolating the effect of the metric upon observed quantities from "secondary physics", e.g. stellar evolution, galaxy merging, etc., and observational biases, e.g. the k–correction, magnitude estimation and sample statistics.

2.1 Definitions of distance, volume and time

Distances, volumes and times in the universe cannot be observed "directly". There is no universal ruler or clock with which to measure such quantities. Therefore, quantities such as distance, etc. are defined in terms of their relationship to observed quantities.

Distances and volumes are defined by considering the path of a photon as it travels through the expanding universe from a distant source to the observer. Photon trajectories in spacetime are referred to as null geodesics which satisfy $\mathrm{d}s^2 = 0$ by definition. We further consider a photon travelling along a purely radial trajectory, i.e. $\mathrm{d}\theta = \mathrm{d}\phi = 0$. Returning to the RW line element we may therefore write

$$\begin{aligned} c\ \mathrm{d}t &= \frac{a(t)\ \mathrm{d}r}{\sqrt{1-kr^2}} \\ \frac{c\ \mathrm{d}t}{a(t)} &= \frac{\mathrm{d}r}{\sqrt{1-kr^2}}. \end{aligned} \tag{1}$$

In considering a photon emitted at coordinates $(t = t_1, r = 0)$ and received at $(t = t_0, r = r)$ we generate the following integral

$$\int_{t_1}^{t_0} \frac{c\ \mathrm{d}t}{a(t)} = \int_0^r \frac{\mathrm{d}r'}{\sqrt{1-kr'^2}} \tag{2}$$

The coordinate radius describing the co-moving distance between the source and observer is defined as

$$S(r) = \int_0^r \frac{\mathrm{d}r}{\sqrt{1-kr^2}}. \tag{3}$$

Evaluating $S(r)$, one obtains

$$\begin{aligned} S(r) &= \arcsin r \quad \text{for} \quad k = +1, \\ &= r \quad \text{for} \quad k = 0, \\ &= \operatorname{arcsinh} r \quad \text{for} \quad k = -1. \end{aligned} \tag{4}$$

The physical radius giving the source-observer separation at a particular epoch, t, is $a(t)\ S(r)$. Therefore, as we shall see below, when we consider the distance between objects in an expanding universe, we must also consider the time evolution of the scale factor. This leads us to evaluate the integral presented in Equation 2.

2.1.1 Angular diameter distance

Angular diameter distance, d_A, is defined as the ratio of an object's physical transverse size to its apparent angular size (in radians). For an object of fixed (not expanding with the Hubble flow) transverse size, y, and apparent angular size, $\delta\theta$, the angular diameter distance to the object is defined as

$$d_A = y/\delta\theta. \tag{5}$$

For two photons emitted at a time, t_1, from either end of the object, the light paths are defined by two close, radial null geodesics (Figure 1). In this case, the transverse size (or length) of the object is simply $\delta\theta$ multiplied by the radial distance to the observer as calculated at the time of emission, i.e.

$$y = \delta\theta \times a_1 S(r) \quad \text{or} \quad \frac{y}{\delta\theta} = a_1 S(r). \tag{6}$$

However, recalling $a_0/a_1 = 1 + z$, one obtains

$$d_A = a_0 S(r)/1 + z. \tag{7}$$

The angular diameter distance is therefore obtained from the solution to Equation 2. Note that the solution to this general integral will be discussed after all of the distance/volume measures have been defined.

2.1.2 Luminosity distance

Luminosity distance is defined such that the ratio between bolometric luminosity and the observed bolometric flux of a given object is

$$d_L = \sqrt{\frac{L_{bol}}{4\pi f_{bol}}}. \tag{8}$$

The radiation from this object reaches us having travelled a radial distance $a_0 S(r)$ and is distributed over a pseudo–spherical surface (of constant time) of surface area $4\pi(a_0 S(r))^2$. However, two additional factors are required.

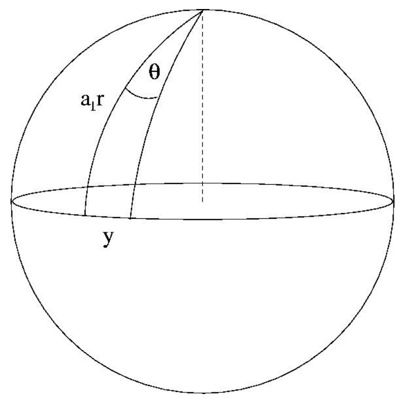

Figure 1: The angle between radial light paths in a 2-dimensional curved universe

1. The energy of each photon decreases proportionally with the redshift factor,

$$E_{\gamma,0} = h\nu_0 = \frac{h\nu_e}{1+z}. \tag{9}$$

2. The rate of reception of photons (remember we are dealing with a flux here) decreases by a further factor $1+z$ if one considers that $\Delta t_0/\Delta t_e = a_0/a_e = 1+z$.

Therefore, the original flux versus luminosity relation may be re–written as

$$f_{bol} = \frac{L_{bol}}{4\pi(a_0 S(r))^2 (1+z)^2}, \tag{10}$$

i.e. $d_L = (a_0 S(r)) \cdot (1+z)$. Note that $d_L = (1+z)^2\ d_A$. We have so far restricted the discussion of luminosity distance to bolometric quantities. The k–correction must be considered when dealing with **spectral** flux and luminosity and will be discussed later.

2.1.3 Co–moving volume

The co–moving volume defines a region of the universe in which the number density of non–evolving objects expanding with the Hubble flow is constant with redshift. The co–moving volume computed over the full sky out to a radial coordinate r is therefore,

$$V_c = 4\pi a_0^3 \int_0^r \frac{r'^2 \mathrm{d}r'}{\sqrt{1-kr'^2}}. \tag{11}$$

2.2 Solving for distance versus redshift

General solutions to the distance versus redshift relations are best given by Hogg (astro–ph/9905116). However, the analytic solutions for an EdS universe with $k = 0$ are given here. Recall that the solution for the term $a_0 S(r)$, involved in the computation of d_L, d_A, and V_c, is based upon the following relation obtained from the RW line element

$$\int_{t_e}^{t_0} \frac{c\ \mathrm{d}t}{a(t)} = \int_0^r \frac{\mathrm{d}r'}{\sqrt{1-kr'^2}}. \tag{12}$$

For $k = 0$ the RHS of this equation reduces to r. Taking the LHS one obtains

$$\begin{aligned}
\int_{t_e}^{t_0} \frac{c\ \mathrm{d}t}{a(t)} &= \frac{c\ t_0^{2/3}}{a_0} \int_{t_e}^{t_0} \frac{\mathrm{d}t}{t^{2/3}} \longleftarrow \left[\frac{a(t)}{a_0} = \left(\frac{t}{t_0}\right)^{2/3}\right] \\
&= \frac{3\ c\ t_0^{2/3}}{a_0}\ [t^{1/3}]_{t_e}^{t_0} \\
&= \frac{3\ c\ t_0^{2/3}}{a_0}\ [t_0^{1/3} - t_e^{1/3}]\ \ (\text{note that } (t_0/t_e)^{2/3} = 1+z) \\
&= \frac{3\ c\ t_0^{2/3}}{a_0} \left[t_0^{1/3} - \frac{t_0^{1/3}}{\sqrt{1+z}}\right] \\
&= \frac{3\ c\ t_0}{a_0} \left[1 - \frac{1}{\sqrt{1+z}}\right] \\
a_0 r &= \frac{2c}{H_0} \left[1 - \frac{1}{\sqrt{1+z}}\right] \longleftarrow \left[t_0 = \frac{2}{3} H_0^{-1}\right].
\end{aligned} \tag{13}$$

Returning to the previous geometric definitions, we can now write explicit distance and volume formulae for the EdS case, i.e.

Angular diameter distance:

$$d_A(z) = \frac{2c}{H_0}\ \frac{1}{(1+z)}\ \left[1 - \frac{1}{\sqrt{1+z}}\right]. \tag{14}$$

Luminosity distance:

$$d_L(z) = \frac{2c}{H_0}\ (1+z)\ \left[1 - \frac{1}{\sqrt{1+z}}\right]. \tag{15}$$

Co–moving volume element:

$$V_c = 4\pi a_0^3 \int_0^r \frac{r'^2 \, \mathrm{d}r'}{\sqrt{1 - kr'^2}}. \tag{16}$$

For $k = 0$, $V_c = 4\pi/3 \cdot (a_0 r)^3$, therefore

$$V_c = \frac{32\pi}{3} \left(\frac{c}{H_0}\right)^3 \left(1 - \frac{1}{\sqrt{1+z}}\right)^3. \tag{17}$$

Note that this volume is computed over the full sky, i.e. 41,253 deg^2 or 4π Sr.

It is then simple to define the **differential** co-moving volume element as

$$\frac{\mathrm{d}V_c}{\mathrm{d}z}\mathrm{d}z = V_c(z + \mathrm{d}z) - V_c(z). \tag{18}$$

2.2.1 Look back time

The look back time is the difference in the age of the universe between the epochs of photon emission and observation, i.e. $t_L = t_0 - t_1$. For specific cases one may solve this equation directly. For example, for the EdS case, i.e. $k = 0$, $a \propto t^{2/3}$, we can write

$$\begin{aligned} t_L &= t_0 - \left(\frac{a_1}{a_0}\right)^{3/2} t_0 \\ &= t_0 \left(1 - \frac{1}{(1+z)^{3/2}}\right) \\ &= \frac{2}{3} H_0^{-1} \left(1 - \frac{1}{(1+z)^{3/2}}\right), \end{aligned} \tag{19}$$

recalling that $t_0 \simeq 2/3 H_0^{-1}$.

2.3 Characteristic scales

The above equations introduce a characteristic universal distance and volume in addition to the characteristic time discussed in Lecture 1:

$$\begin{aligned} \text{Hubble distance} &\equiv \frac{c}{H_0} = 3000 \; h^{-1}\mathrm{Mpc} \\ \text{Hubble volume} &\equiv \left(\frac{c}{H_0}\right)^3 = 2.7 \times 10^{10} \; h^{-3}\mathrm{Mpc}^3 \\ \text{Hubble time} &\equiv \frac{1}{H_0} = 9.78 \times 10^9 \; h^{-1} yr, \end{aligned} \tag{20}$$

where $H_0 = 100 \; h$ kms^{-1} Mpc^{-1} introduces a useful "cosmology free" unit.

2.4 Toward observational tests

The variation of d_A, d_L and V_c with redshift are dependent – in a unique manner – upon the combination of Ω_0, Λ_0 and H_0 (we consider only matter dominated universes at present). Immediately, three observational approaches are evident:

1. Observe a population of objects of fixed physical size with increasing redshift to determine the form of $d_A(z)$ (or $d_A(z, \Omega_0, \Lambda_0, H_0)$).

2. Observe a population of objects of fixed absolute luminosity with increasing redshift to determine $d_L(z)$.

3. If one can first determine the luminosity function of a population of objects, measuring the galaxy number distribution as a function of apparent magnitude, $N(< m)$, constrains the combination of $d_L(z)$ and $\mathrm{d}V_c/\mathrm{d}z$.

2.5 Mapping $d_L(z)$ via the Hubble diagram

Consider the **distance modulus** equation that relates the apparent magnitude m of a source of absolute magnitude M, viewed at a distance d,

$$m = M + 5 \log \left(\frac{d}{10 \text{ (pc)}} \right) . \tag{21}$$

This equation was originally formulated for stellar (i.e. Galactic) studies. To cast this equation in cosmological form one considers the apparent magnitude variation with redshift, $m(z)$, of a source of absolute magnitude M,

$$m_\lambda(z) = M_\lambda + 25 + 5 \log[d_L(z)] + K_\lambda(z) + E_\lambda(z), \tag{22}$$

where the subscript "λ" indicates that we are now considering **spectral** rather than **bolometric** brightness measures. Several terms require explanation:

1. $25 + 5 \log[d_L(z)(\mathrm{Mpc})]$ is the **cosmological** distance modulus.

2. $K_\lambda(z)$ is the k–correction that accounts simultaneously for the changing rest frame bandwidth and the changing portion of the source spectral energy distribution (SED) sampled with varying redshift (see next section).

3. $E_\lambda(z)$ describes the effect of luminosity evolution with redshift in the source (we will see later how this combines with $K_\lambda(z)$). Note that any "standard candle" that displays a non-zero E_λ term is not standard.

4. Note that an extinction term is not present explicitly. Extinction may be best represented by modifying the rest frame source SED.

2.5.1 The k–correction

Consider the spectral flux f_λ received from a source described by an SED of the form $S(\lambda)$, observed using a filter of spectral response $R(\lambda)$,

$$\begin{aligned} f_\lambda &= \int_0^\infty S(\lambda)R(\lambda)\,\mathrm{d}\lambda, \quad \text{or} \\ M_\lambda &= -2.5\log\left[\int_0^\infty S(\lambda)R(\lambda)\,\mathrm{d}\lambda\right]. \end{aligned} \tag{23}$$

Note that this integral is computed in the observer's frame and recall that the SED units are expressed as [**energy time**$^{-1}$ **area**$^{-1}$ **angstrom**$^{-1}$]. Consider now the same source, observed using the same filter, located at a redshift z. The change in observed magnitude arising from the redshift of the SED w.r.t. the filter may be expressed as

$$\begin{aligned} K_\lambda(z) &\equiv M(z) - M(z=0) \\ &= -2.5\log\left[\frac{\int_0^\infty S(\lambda_{rf}\times 1+z)R(\lambda_{obs})\,\mathrm{d}(\lambda_{obs}/1+z)}{\int_0^\infty S(\lambda_{obs})R(\lambda_{obs})\,\mathrm{d}\lambda_{obs}}\right] \\ &= 2.5\log(1+z) - 2.5\log\left[\frac{\int_0^\infty S(\lambda_{rf}\times 1+z)R(\lambda_{obs})\,\mathrm{d}\lambda_{obs}}{\int_0^\infty S(\lambda_{obs})R(\lambda_{obs})\,\mathrm{d}\lambda_{obs}}\right] \end{aligned} \tag{24}$$

Note the factor of $1+z$ in the dλ term in the numerator. This comes from recalling the SED units. The term [$\mathbf{angstrom_{obs}^{-1}}$] is expressed as [$(\mathbf{angstrom_{rf}} \times \mathbf{1+z})^{-1}$]. This is where the extra factor of $(1+z)$ comes from. For a spectrally flat SED, the second term in Equation 24 equals zero.

2.5.2 The $[e+k](z)$ correction

A number of observational and theoretical studies point to the fact that astronomical sources (here generalised to galaxies – composite stellar populations) evolve with time. Evolution of the spectral flux of a given source may be accounted for by modifying the term $S(\lambda)$ to $S(\lambda, t(z))$. The above k–correction may be re–written as a general, evolution plus k–term, i.e.

$$[e+k](z) = 2.5\log(1+z) - 2.5\log\left[\frac{\int_0^\infty S(\lambda_{rf}\times 1+z, t(z))R(\lambda_{obs})\,\mathrm{d}\lambda_{obs}}{\int_0^\infty S(\lambda_{obs}, t(z=0))R(\lambda_{obs})\,\mathrm{d}\lambda_{obs}}\right] \tag{25}$$

The study of galaxy evolution as an end in itself (rather than as test particles in cosmological tests) developed during the 1970s (see papers by Larson and Tinsley). Early work expressed $E_\lambda(t)$ in forms such as $L \propto t^{-4/3}$, based upon approximations to stellar evolution calculations. However, the advent of isochrone synthesis models (e.g. Bruzual and Charlot 1993 and later papers) using comprehensive stellar spectrum libraries permits $S(\lambda, t)$ to be computed directly.

2.5.3 A few caveats when constructing the Hubble diagram

1. **Malmquist bias**

   Hubble and Humason (1932, 1934) rapidly extended the distance over which the $m(z)$ test could be performed by observing the characteristic, or mean, magnitude of distant clusters and groups of galaxies. However, when computing the mean magnitude of a sample of objects (in the above case assumed to be at the same distance), unless one includes information on the limiting magnitude sensitivity of the survey, m_l, and the magnitude distribution function of the sources (galaxies), $f(m)$, one will systematically **over estimate** the characteristic brightness $\langle m \rangle$ and consequently **under estimate** the distance. For example, consider the case where one defines

$$\langle m \rangle = \frac{\int_{-\infty}^{\infty} m \ f(m) \ \mathrm{d}m}{\int_{-\infty}^{\infty} f(m) \ \mathrm{d}m}, \tag{26}$$

   as $\langle m \rangle$ approaches m_l, $\langle m \rangle$is systematically overestimated (Figure 2). One must instead compute the quantity,

$$\langle m \rangle = \frac{\int_{-\infty}^{m_l} m \ f(m) \ \mathrm{d}m}{\int_{-\infty}^{m_l} f(m) \ \mathrm{d}m}. \tag{27}$$

   Which requires an understanding of m_l and $f(m)$.

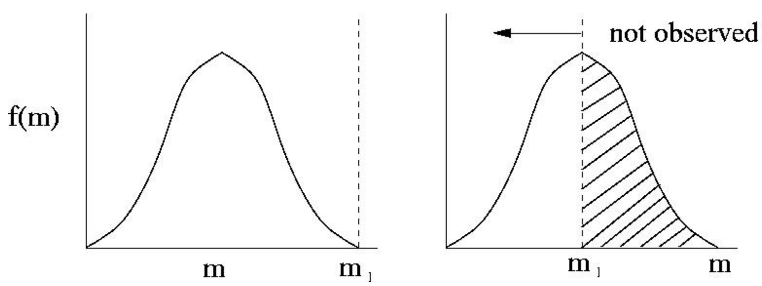

Figure 2: Malmquist bias in action.

2. **Aperture Bias**

   Galaxy magnitudes are typically measured within a fixed angular aperture as viewed on a given image (e.g. CCD frame or photograph). However, this angular aperture corresponds to a varying physical scale in the galaxy rest frame and a varying fraction of the galaxy surface brightness distribution $\mu(r)$ will lie within the observed aperture limits (Figure 3).

   The integrated magnitude of a source may be defined as

$$m = \int_0^{r_{lim}} 2\pi \ r \ \mu(r) \ \mathrm{d}r, \tag{28}$$

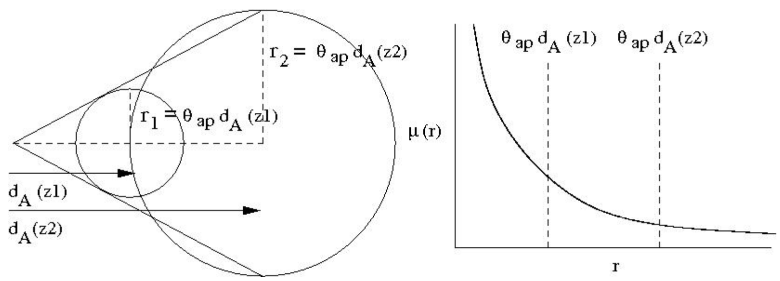

Figure 3: Changing aperture sizes with redshift.

for a circularly symmetric source. The question is then how should one correct the integrated magnitude of a sample of objects observed over a range of redshifts, to a uniform, rest frame physical scale? Different solutions to this problem include

(a) Define a "constant light fraction" radius based upon the radial distribution of light in each object. An example is the Kron radius (Kron 1980). The first image moment (or flux weighted radius) can be computed as $\bar{r} = \sum r_i^2 f_i / \sum r_i f_i$ where r_i is the radial value of each object pixel (measured from the central pixel and f_i is the corresponding flux. Once can then define a circular or elliptical aperture based upon this radius, e.g. setting $r_{Kron} = 2.5 \times \bar{r}$ is claimed to enclose $> 90\%$ of the source flux.

(b) Apply a fixed angular aperture that corresponds to the limiting isophote of the detector image. This is observationally practical as there typically exists one μ_{limit} per image. However, in order to correct all images to a given scale one must integrate the assumed form of $\mu(r)$ out to some (large) radius. This is the idea behind *model* magnitudes. It is particularly effective when one is certain of the model used to describe the surface brightness distribution of the objects, e.g. SNe Ia total magnitudes are computed using a PSF model (also known as PSF-magnitudes).

(c) Apply a fixed metric aperture. An aperture of fixed rest frame scale, $r = \theta_{ap}\ d_A(z)$, is applied to all galaxies. This is suitable for galaxy redshift surveys (say), where redshifts are available for all sources. However, one must assume the form of $d_A(z)$.

(d) Choose θ_{ap} to be sufficiently large such that approximately all the flux from a particular galaxy is received. This is a good calibration technique but aperture sizes are limited in crowded (i.e. deep) images.

3. **Peculiar velocities**

Peculiar velocities arise from galaxy motions along the line of sight toward the observer and are caused by gravitational interactions with the local matter (i.e. galaxy) distribution. Peculiar velocities are not associated with the Hubble flow. Peculiar velocities appear as an additional term in the observed redshift,

$$cz_{obs} = v_{pec}(1 + z_{cosm}) + cz_{cosm}, \tag{29}$$

where v_{pec} is considered in the galaxy rest frame. Locally, one may re–write the Hubble relation as

$$v_{rec} = H_0\ d + v_{pec}. \tag{30}$$

Therefore, correct determination of the local galaxy velocity field is crucial to determining an unbiased value of H_0. Peculiar velocities are manifest in a number of observations:

(a) The local group: within a few Mpc of the Milky Way, the kinematic properties of the local group (LG) of galaxies (dominated by the Milky Way and M31) dominate over the Hubble flow. Radial velocity measurements of LG members permit accurate orbits to be computed in a fairly straightforward manner.

(b) The local velocity field: physical distances to local spiral and elliptical galaxies may be obtained via Tully–Fisher and $D_n - \sigma$ relations. Having measure the observed redshift, peculiar radial velocities may be computed and the velocity field obtained via integration. Analyses such as this indicate that the LG is falling towards the Virgo cluster of galaxies (approximately 15 Mpc distant) with a velocity of 250 kms^{-1}.

(c) Motion of the LG w.r.t. the CMB: analysis of the CMB dipole indicates that the bulk motion of the LG w.r.t. the CMB is $v_{CMB} = 606$ kms^{-1} toward the direction $l = 268°, b = 27°$.

(d) Redshift space distortions – the "Finger of God" effect: redshift observations of massive galaxy clusters (virialised systems of galaxies with apparently discrete spatial boundaries) appear elongated along the radial axis in redshift versus sky projection plots. This phenomenon arises from the well–defined distribution of orbital velocities within the cluster being superposed upon the Hubble flow.

2.5.4 The Hubble diagram test in practice

The $m(z)$ test is observationally challenging – redshifts must be secured for distant, "standard candle" sources. Differences in $d_L(z)$ for difference cosmological models only become appreciable (or measurable by practical means) at large redshifts (i.e. $z > 0.5$). At such distances, typical sources become very faint and redshift determination is challenging. A menagerie of standard candles has and continues to be used to approach this problem:

- Novae
- Cepheids – excellent distance indicator, though not visible to "cosmological" distances
- Brightest galactic star

- Characteristic magnitude of cluster galaxy magnitude distribution
- Brightest, or "first ranked", cluster galaxies
- Radio galaxies
- Tully–fisher relation for spirals ($L \propto v_c$)
- Tip of red giant branch
- Supernovae Type Ia (SNe Ia) – currently a highly favoured standard candle

How standard should a "standard candle" be? Ideally, absolute magnitude variations within a given class of object should be significantly smaller than variations in the cosmological distance modulus for the cosmological models of interest. In practice, many of the above standard candles do not satisfy this criterion due to physical evolution and observational biases.

We focus on two standard candles that have passed the test of time: Cepheid variable stars and Type Ia supernovae.

Cepheid variable stars are hyper luminous giant stars with luminosities in the range $\bar{L} = 400 \rightarrow 40,000 L_\odot$. Cepheids are pulsationally unstable: as they pulse radially the total luminosity varies due to the changing surface area and temperature of the photosphere. Pulsation periods lie in the range $P = 1.5 \rightarrow 60$ days. The range in luminosity demonstrated by Cepheids would preclude their use as a standard candle were it not for a well-defined **period-luminosity** relation governing the period P and the mean flux $\bar{f}$ (or luminosity $\bar{L}$) emitted over one period. This relationship was defined observationally for Cepheids in the Small Magellanic Cloud (SMC), i.e. it was initially a period-flux relationship but, assuming all Cepheids in the SMC to be at the same distance (and once you obtain the distance to the SMC using "secondary" indicators[1]) it becomes a period-luminosity relation. Consider the observation of two Cepheid variable stars of period 10 days – one in the Large Magellanic Cloud (LMC) and one in M31 (Andromeda). Observation yields the result

$$\frac{\bar{f}_{LMC}}{\bar{f}_{M31}} = 230, \tag{31}$$

from which one can conclude that the ratio of the luminosity distances is

$$\frac{d_L(M31)}{d_L(LMC)} = \left(\frac{\bar{f}_{LMC}}{\bar{f}_{M31}}\right)^{1/2} = \sqrt{230} = 15.2. \tag{32}$$

Subsequent secondary distance indicators provide $d_L(LMC) = 50 \pm 3$ kpc from which one infers that $d_L(M31) = 760 \pm 50$ kpc.

[1]This was achieved using a combination of main-sequence fitting and secular parallax distances.

One of the main reasons for constructing the Hubble Space Telescope (HST) was to measure Cepheid variable stars out to luminosity distances $d_L \sim 20$ Mpc in order to determine an accurate value for the the Hubble constant. Consideration of Hubble's law indicates that 20 Mpc corresponds to a very small redshift. Looking back at the form of the luminosity distance versus redshift relation (Equation 15) one notes that at $z \ll 1$ all redshift terms vanish. Therefore, the measurement of H_0 is not affected by any ignorance of history of the scale factor (e.g. acceleration or deceleration). However, observing Cepheids out to 20 Mpc still places them within the "local" universe where deviations from the Hubble flow arising from peculiar velocities (e.g. from Virgo) will bias any measurement. Measurements of individual Cepheid redshifts (velocities) must be corrected for the local velocity field. The value of H_0 determined by the HST Key Project team is 75 ± 8 kms^{-1}Mpc^{-1}.

Type Ia supernovae are a specific sub-class of exploding stars that display exceptionally uniform peak luminosities. Supernovae classes were initially defined observationally: Type II supernovae display hydrogen lines in their spectra, Type I do not. Type II supernovae are massive stars ($M > 8\mathrm{M}_\odot$) whose cores collapse to form a neutron star or black hole when nuclear burning can no longer support the star. Further observation indicated that Type Ib supernovae were similar to Type II's with the exception that the hydrogen in the stellar envelope has been blown away prior to collapse. Type Ia supernovae appear to be fundamentally different. They are thought to originate in binary systems containing a massive star accreting onto a white dwarf companion. When the growing mass of the white dwarf passes the Chandrasekhar limit (1.4 $\mathrm{M}_\odot$) the white dwarf collapses under its self-gravity with the effect that the density increases to the point where internal nuclear fusion re-commences and the star is consumed in a well-calibrated nuclear explosion.

Type Ia supernovae are very bright and have been observed to redshifts $z = 1.7$. The typical peak brightness of a Type Ia supernova is $L = 4 \times 10^9 L_\odot$ – about $M_V = -19.2$. Type Ia supernovae can therefore be observed well beyond the region of the universe that is locally flat to greater distances where the effect of space curvature (matter and dark energy) are important. All of these observations are part of a "distance ladder" and, taking the distance to the Virgo cluster measured using Cepheids, the value of H_0 determined using SNe Ia is 70 ± 7 kms^{-1}Mpc^{-1}.

2.6 The number–magnitude test – $N(m)$: Are galaxies distributed uniformly in space?

In contrast to the Hubble diagram test, the $N(m)$ test is observationally easier to construct. Images of apparently blank regions of the sky provide an unbiased sample of the galaxy distribution. Such "blank field" observations may extend to large areas (to sample a greater number of galaxies) and faint magnitude limits (to sample more distant galaxies and to increase the sensitivity to cosmological parameters). However, the dependence of $N(m)$ upon cosmological parameters is more complex than the $m(z)$ test and involves additional physics such as the luminosity function (LF) as a function of galaxy type.

In the local universe one may consider the $N(m)$ distribution of galaxies distributed uniformly in space and displaying a fixed luminosity L. In this case (remember that **local** is akin to saying **spatially flat**)

$$f = L/4\pi l^2, \tag{33}$$

is the apparent brightness of a galaxy at a distance l. For a uniform number density of galaxies, n, the total number brighter than f is

$$N(>f) = \frac{4}{3}\pi l^3 n = \frac{4}{3}\pi n \left(\frac{L}{4\pi f}\right)^{3/2} \propto f^{-3/2}. \tag{34}$$

Employing the relation, $f \propto 10^{-0.4m}$, one may re–write the above relationship as

$$\log N(<m) = 0.6m + \text{constant}. \tag{35}$$

As the original relationship may be written as $\mathrm{d}f = \mathrm{d}L/4\pi l^2$, the above analysis is applicable to a population of objects described by some general LF.

Hubble (1926) and Shapley & Ames (1932) confirmed that this relation holds to $m_{pg} \sim 18$ and thus that galaxies are distributed uniformly in local space – which in turn may be considered as spatially flat. This was the first direct indication that galaxies are reliable tracers of the wider universe. Though large scale structures (e.g. galaxy clusters) do exist, if one averages over a large enough region of space, a uniform distribution results. In contrast to this, a similar analysis was employed to assess $N(m)$ for stars in the Galaxy. The above relation does not hold, indicating that the Galaxy (as traced by stars) is limited in space. From the initial results of Hubble and Shapley & Ames, the $N(m)$ test was extended to fainter magnitude limits in order to detect any deviation from the $N(m)$ relation predicted for a spatially flat universe. Could the signature of space curvature be detected?

To compare observed $N(m)$ values to values predicted for a general cosmology and galaxy population model, one must construct a relation of the form

$$N(m)\ \mathrm{d}m|_{T=all} = \sum_i \int_m^{m+\mathrm{d}m} \int_0^\infty \phi(m(M,z),T_i,z)\ \frac{\mathrm{d}V_c}{\mathrm{d}z}\ \mathrm{d}m\ \mathrm{d}z, \tag{36}$$

where $N(m)\ \mathrm{d}m|_{T=all}$ is the number of galaxies occupying the apparent magnitude interval m to $m + \mathrm{d}m$, summed over all galaxy types. The quantity $\phi(M,T,z)$ is the galaxy LF considered as a function of absolute magnitude, galaxy type and redshift.

2.6.1 Eddington bias

Eddington bias described the effect of observational uncertainty in m upon the form of the $N(m)$ relation. Consider an ideal $N(m)$ relation where $N(m)$ increases monotonically with increasing m. If one convolves this relation with a Gaussian error in m of the form

$$f(m)\ \mathrm{d}m = Ae^{-[(m-\bar{m})^2/2\sigma^2]}, \tag{37}$$

where σ is the observed error, then galaxies within a particular m to $m + \mathrm{d}m$ interval are scattered into neighbouring intervals. However, as $N(m)$ increases to faint m, any particular magnitude "bin" receives more galaxies scattered from fainter magnitude bins that from brighter ones (figure 4). The observed $N(m)$ relation is shifted systematically to brighter magnitudes.

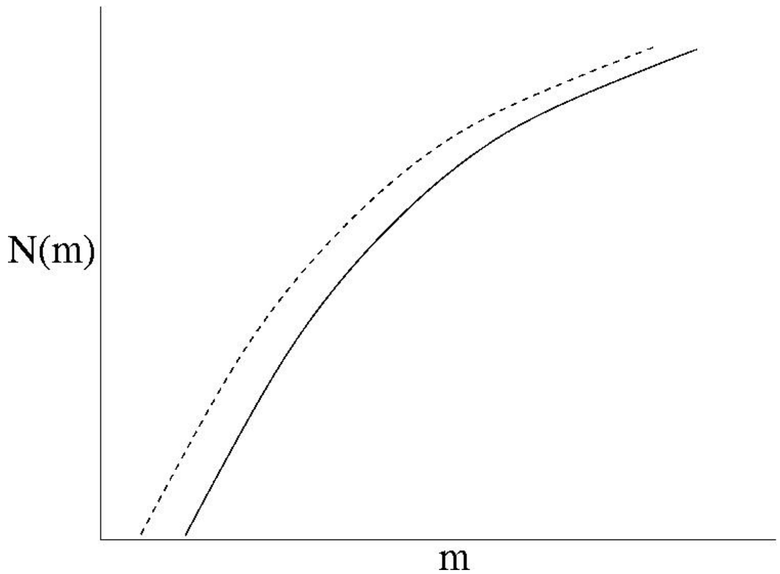

Figure 4: The effect of Eddington bias on the N(m) relation.

To account for this effect in the predicted $N(m)$ relation, one replaces $\phi(m)$ with $\phi_{obs}(m)$ where

$$\phi_{obs}(m) = \frac{1}{\sqrt{2\pi}\sigma} \int_{-\infty}^{\infty} \phi(m')\; e^{-(m'-m)^2/2\sigma^2}\; \mathrm{d}m', \tag{38}$$

expresses analytically a Gaussian smoothing of the galaxy LF.

2.6.2 The history of the $N(m)$ test

Following the early observations of Hubble and Shapley & Ames, considerable observational effort was expended in extending the $N(m)$ test to fainter apparent magnitudes. Surveys were performed using photographic plates with telescope + camera combinations offering large fields of view (e.g. Schmidt plate surveys). Though CCDs were available from the early 1980's onwards, their restricted fields of view (FOVs) did not permit large area $N(m)$ studies (low area = cosmic variance) despite providing greatly enhanced sensitivity. However, all tests of the cosmological model using the $N(m)$ relation were eventually undermined by the realisation that the effects of galaxy evolution – parameterized by the $[e+k](z)$ and $\phi(z)$ terms – dominated over the effects of a varying cosmological model (i.e. $d_L(z)$ and $\mathrm{d}V_c(z)$) at redshifts where the $N(m)$ test was applicable.